Chapter 4

Experiment

X-ray magnetic circular dichroism combined with photoelectron emission microscopy, XMCD-PEEM, is a powerful tool to investigate local magnetization in ferromagnetic layers separately in multilayered systems. Up to now, lateral- and elemental-resolved studies of magnetic multilayered systems have been performed prosperously and reported in Refs. [49–53]. The observation of magnetization reversal dynamics with element selectivity has been performed by XMCD with a pump-probe technique, but without lateral resolution [54, 55]. Temporally resolved magnetic domain imaging in single magnetic layers has been done mainly using Kerr microscopy in the picosecond range [56–60] and in the second range [9–11, 44]. Magnetization reversal in the second range has been studied using XMCD-PEEM in Section 5.1.

In this thesis, the ns time-, lateral- and elemental-resolved experiment by a novel combination of XMCD-PEEM and a pump-probe technique has been successfully performed. Using this technique, I have studied how micro-magnetic effects act on magnetization reversal dynamics of magnetic multilayered systems (SV and MTJ like trilayers) in the ns time scale. Evolution of the magnetic domain structure in a magnetically soft layer of such trilayers by separate ns-long field pulses was observed, so called single-pulse experiment.

In Section 4.1, the technique of magnetic domain imaging with element selectivity is briefly explained. The usage of the micro-coil is described in Section 4.2.

4.1 Magnetic domain imaging with element selectivity: XMCD-PEEM

4.1.1 X-ray Magnetic Circular Dichroism

X-ray Magnetic Circular Dichroism, XMCD, is the difference of absorption intensities by changing either the helicity of incoming circularly polarized x-rays or the magnetization of a specimen. It

is simply explained in the following section by a two-step model, by considering the transition of electrons from a 2p core state to a 3d valence state in a 3d transition metal [61]. All excited electrons from the 2p state are assumed to be transferred to the 3d valence state. Excitation by either magnetic scattering or Compton effect are negligible.

Two-step model

The first step is the excitation of electrons from the 2p core state by circularly polarized x-rays. In Fig. 4.1, schemes of electron excitations from the $2p_{3/2}$ state to the 3d valence state in a 3d transition metal by circularly polarized x-rays are shown. The magnetization of the sample is reversed between (a) and (b). Because of the spin-orbit interaction, the 2p core state splits into two levels, $2p_{3/2}$ and $2p_{1/2}$, and the coupling between spin and angular momenta on these levels are opposite, l + s and l – s, respectively, where l and s are the orbital and spin angular momenta. The energy separations between these two states are 13.1, 15.1 and 17.3 eV for Fe, Co and Ni, respectively. The photon energy of circularly polarized x-rays is tuned to excite electrons from $2p_{3/2}$ state to the high density of unoccupied 3d states just above the Fermi level. Now let's assume the x-ray is circularly polarized. and spin-up electrons are mainly excited, while, spin-down electrons are excited less. In this process, the polarization of electron spins is conserved. The ratio of excitation probability

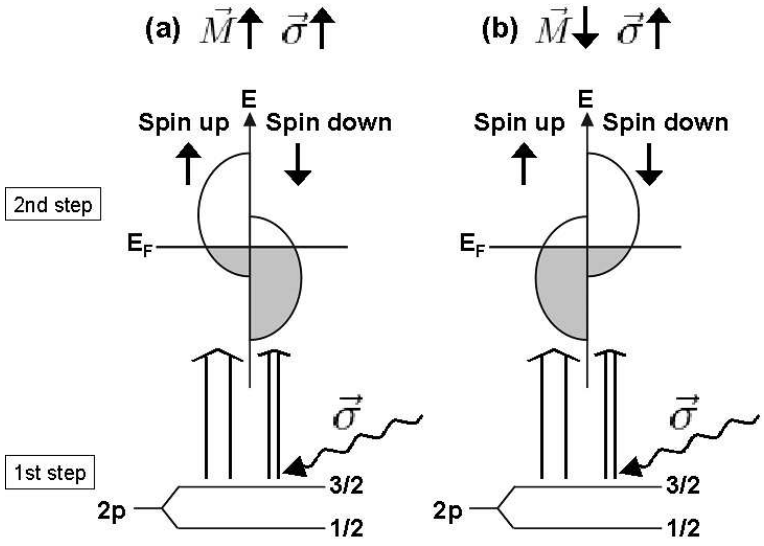

Figure 4.1: Schematic picture of the electron transition from the $2p_{3/2}$ to the 3d states in a 3d transition metal, when the helicity of circularly polarized x-ray and the magnetization of the specimen are parallel (a) or antiparallel (b). A product of the ratio of excited electrons with up- and down-polarizations (indicated by open arrows) and the ratio of up- and down-unoccupied states will be different between (a) and (b), which gives the dichroism.

of spin-up and spin-down electrons is the same for (a) and (b) in Fig. 4.1. On the contrary, if the photon energy is turned to the L_2 absorption edge, spin-down electrons will be mainly excited.

The second step is the detection of the excited and polarized electrons by the imbalanced unoccupied spin-up and -down states of 3d character. This imbalance is due to the exchange splitting (Stoner model). In the case of Fig. 4.1 (a), where $\vec{\sigma}$ and $\vec{M}$ are parallel, mostly spin-up electrons are excited as mentioned above, and most of them are accepted by the spin-up unoccupied state. Spin-down electrons are excited less and accepted less.

In case $\vec{M}$ and $\vec{\sigma}$ are antiparallel (Fig. 4.1 (b)), here the magnetization of the sample is reversed, still mainly spin-up electrons are excited, but less detected by the 3d state, because the number of unoccupied states is reversed between spin-up and spin-down states. As a consequence, the total number of electrons making a transition in Fig. 4.1 (a) is larger than in the case of Fig. 4.1 (b). The transition rate will be calculated by a product of the excitation probability and the imbalance of 3d unoccupied states. The same ratio of the number of transferred electrons will be obtained by changing the helicity of the incoming circularly polarized x-rays instead of the reversal of the magnetization.

4.1.2 Photoelectron emission microscopy

The scheme of PEEM produced by Elmitech Gmbh [62,63] and by Focus Gmbh [64,65] are shown in Fig. 4.2 and Fig. 4.3, respectively. These two PEEMs are compared in Table 4.1. In Fig. 4.3, a picture of the micro-coil is also drawn.

	Elmitech PEEM	Focus PEEM
Type of lenses	Magnetic lenses	Electrostatic lenses
Sample potential	0 - –20 keV (–20 keV is used)	Grounded (Micro-coil can be mounted)
Objective lens potential	Grounded	0 - 15 keV (12keV is used)
X-ray incidence angle from sample surface	17 °	30 °
Size of Apertures	30, 70, 110, 500 and 1200 μm (30 μm is used)	30, 70, 150, 500 and 1200 μm (70 μm is used)
Lateral resolution	$\sim$100 nm	$\sim$300 nm

Table 4.1: Comparison between Elmitech PEEM and Focus PEEM.

Elmitech PEEM

In this study an Elmitech PEEM installed on beamline X11SIM in the Swiss Light Source has been used to investigate the formation of stripe domains and the slow motion of the domain walls close to the spin reorientation transition line in a Co/Ni double layer grown on a clean Cu(001) surface (Section 5.1). The top view of the PEEM is drawn in Fig. 4.2. The synchrotron x-rays hit the sample with 17 ° grazing angle from the sample surface. Emitted electrons and photoelectrons are accelerated to the objective lens by applying –20 keV to the specimen, and their directions are deviated towards the camera by the beam separator. The photoexcited electrons pass five magnetic lenses, and the number of them is amplified by the microchannel plate, then the electrons are detected by the CCD camera. Since each lens has a deflector, the course of the electrons can be well aligned. In order to optimize the lateral resolution, one of five different size of apertures, 30, 70, 150, 500 and 1200 μm, is selected. In this study the 30 μm-aperture in diameter was used, and the achieved lateral resolution was $\sim$100 nm. In this PEEM instrument, a compensation coil is mounted to compensate the out-of-plane component of the stray field from the magnetic lenses, but it is not possible to eliminate completely the residual field at sample position. Due to this fact, an epitaxially grown Co film on Cu(001) surface at the sample position in the PEEM had a single magnetic domain.

Using the electron gun (shown in Fig. 4.2) in Low Energy Electron Microscopy (LEEM) mode, surface atomic steps could be observed.

Focus PEEM

The Focus PEEM (Fig. 4.3) connected to either beamline UE56/2-PGM2 or UE52-SGM twin helical undulator beamlines at BESSY in Berlin has been used to study magnetization reversal in the ns range using the micro-coil (see also Fig. 4.3, details in Section 4.2). The specimen is positioned at about 2 mm distance from the objective lens. A maximum of 15 keV can be applied to the objective lens to accelerate the electrons emitted from the specimen. The specimen is on ground potential. The electrons pass through the octpole stigmator/deflector and the three electro-static lenses. The combination of these three lenses ensures a wide choice of the field of view ranging between 5 μm and 500 μm. The electrons reach the imaging unit consisting of two microchannel plates and an aluminium covered YAG crystal in front of the CCD camera. Contrast apertures can be positioned on the optical axis in the plane containing the diffraction pattern. In order to optimize the image contrast and lateral resolution, one of five different size of apertures, 30, 70, 150, 500 and 1200 μm, is selected. In this study, the 70 μm-aperture in diameter was used, and the achieved lateral resolution was $\sim$300 nm. The sample can be moved by 4×4 mm^2 in the surface plane, and is also rotatable in the sample surface plane. The whole apparatus was tilted 30

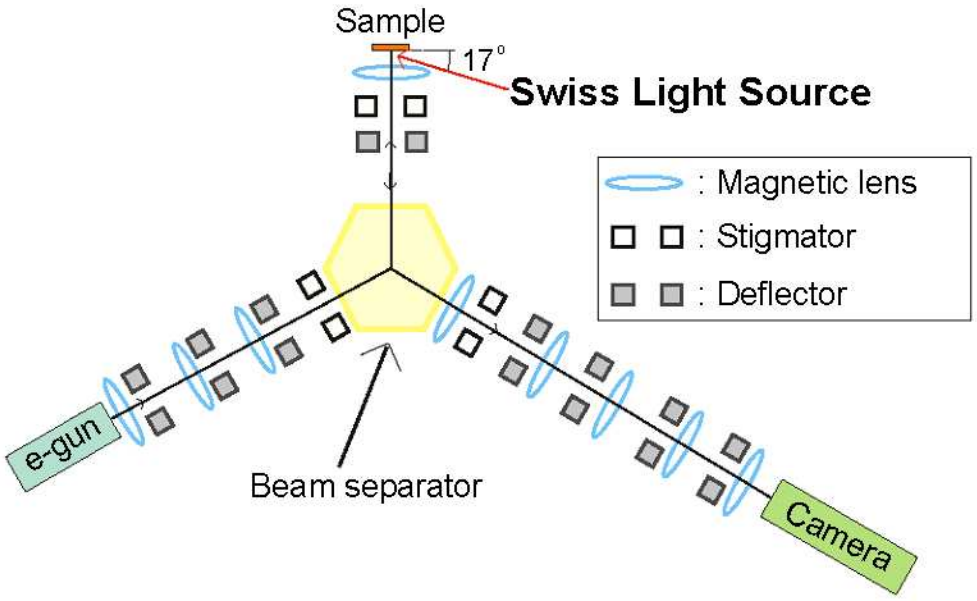

Figure 4.2: Diagram of the PEEM from Elmitech GmbH (Top-view).

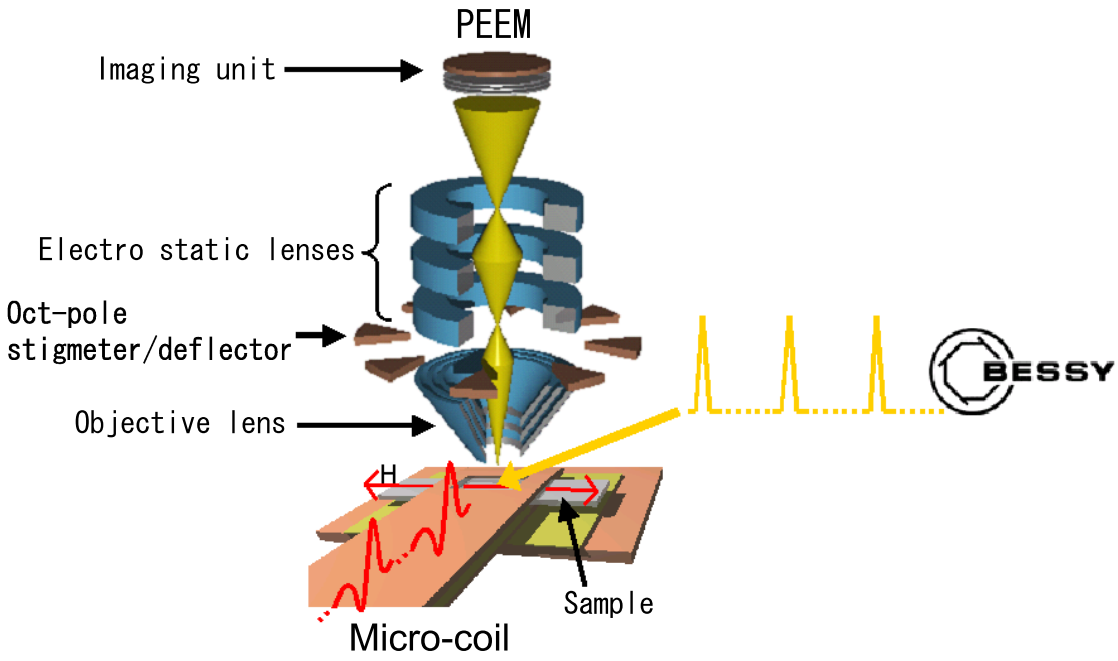

Figure 4.3: PEEM from Focus GmbH and the micro-coil.

° from the vertical axis, so the x-rays hit the sample with a grazing angle of 30° from the sample surface. The PEEM used here was the same as the one used in Refs. [49, 50, 66].

4.1.3 XMCD-PEEM

Fig. 4.4 (a) and (b) show the absorption spectra at the Fe-L_3 and -L_2 edges and on the Co-L_3 edge with positively circularly polarized x-ray (σ^+), respectively, from a MTJ like magnetic trilayer system (3 nm Al/4 nm FeNi/2 nm Al_2O_3/7nm Co/3 nm CoO/Si(111) shown in Fig. 5.21), using the Focus PEEM at the UE56/2-PGM2 twin helical undulator beamline in BESSY. These spectra were obtained by integrating the intensity in the field of view of the XMCD-PEEM images. The Co-L_2 edge is invisible and the background is not flat, because the Co layer of this sample is buried under 9 nm of other material, leading to a low signal-to-background ratio. The sample is identical to the one that will be introduced in Section 5.5.

The magnetic domain structure in the FeNi (c) and the Co (d) layers could be observed sepa-

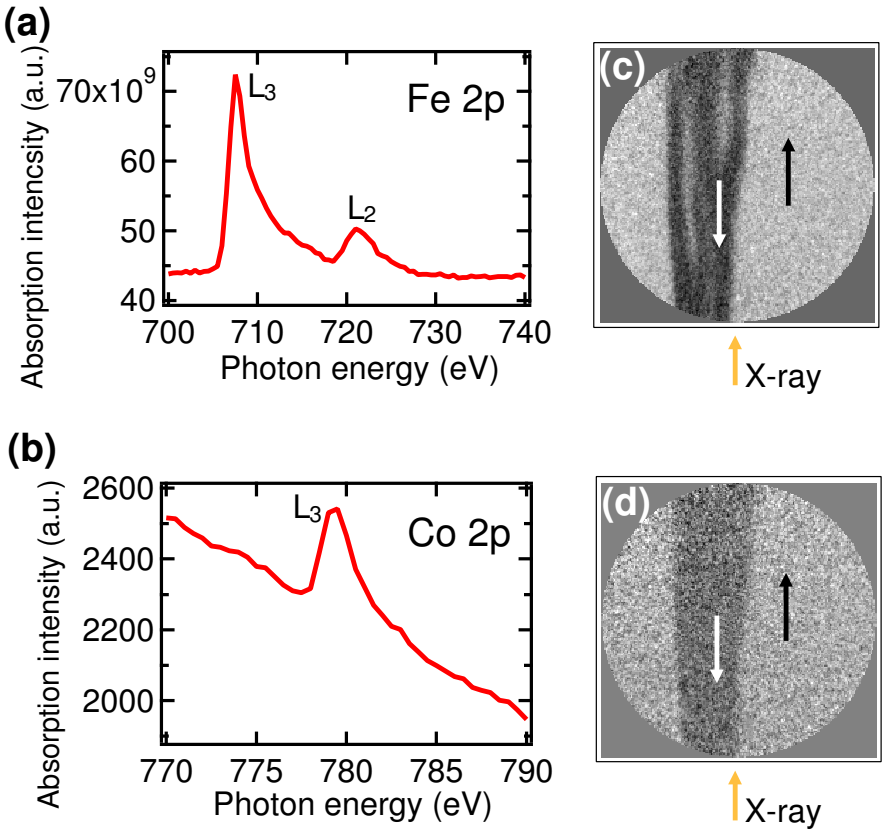

Figure 4.4: X-ray absorption spectra from an MTJ like trilayer system (the sample is shown in Fig. 5.21 in Section 5.5.1) for the Fe-$L_{2,3}$ (a) and Co-$L_{2,3}$ (b) edges. (c) and (d) are the magnetic domain structures in the FeNi and the Co layers obtained by tuning the photon energies to the Fe-L_3 and Co-L_3 edges, respectively. The grey contrast in the images represents the projection of the magnetization direction in the films on the helicity vector of the incoming x-rays indicated by arrows.

rately by tuning the photon energy of the circularly polarized x-rays to the Fe-L_3 and the Co-L_3 edges, respectively. These images are the same as (a) and (h) in Fig. 5.26. The images were created by calculating the asymmetry of two images (difference over sum), which were taken with positive and negative helicity of the circularly polarized x-rays. The grey scale contrast of the PEEM images is proportional to a sine of the angle between the polarization of the incoming circularly polarized x-rays and the local magnetization direction in the film. The local magnetization directions of each film and the direction of incoming x-rays are indicated by arrows. White and dark domains indicate that the magnetization points up and down in the images, respectively.

Since the intensity of secondary electrons is directly proportional to the intensity of photoelectrons, for imaging domain structures the secondary electrons were mainly detected.

4.2 Using a micro-coil

The micro-coil was mounted to the sample in the PEEM, as schematically shown in Fig. 4.3. It is made from a 12.5 μm-thick and 2 cm-wide Cu foil. The x-rays hit the sample inside a hole (0.5×2 mm^2) in the top winding of the micro-coil. Electric current flows through the upper foil, turns around the sample and flows back through the bottom foil, or floes the other way around. This current leads to the generation of magnetic field pulses at the sample position, in the direction indicated by the double arrow. The field direction was in the same vertical plane as the incoming x-rays. The field amplitude was calibrated by Faraday effect measurements with a transparent paramagnetic sample in air. The small piece of transparent paramagnetic material was put into the coil instead of the sample, and a HeNe laser passed through from right to left in Fig. 4.3. The estimated systematic error of the field calibration is $\pm$10 %, as described in Ref. [17].

Using the micro-coil, a variety of experiments could be done. Single-pulse measurements and stroboscopic pump-probe measurements were performed with various pulse lengths and amplitudes. These were adjustable from a few ns to 120 ns and up to 10 mT, respectively. Furthermore, it was possible to select either a monopolar pulse or a bipolar pulse. In single-pulse measurements, the evolution of magnetic domain structures after application of each pulse were observed.

With the pump-probe experiments, the dynamics of the magnetic domain structure induced by the field pulse can be observed. The stroboscopic pump-probe scheme is shown in Fig. 4.5. The pump is the periodic magnetic field pulse created by the micro-coil. The probe is a circularly polarized synchrotron x-ray pulse from BESSY in the single bunch mode of operation. The photon pulses hit the sample every 800 ns. However, only one out of four photon pulses were used and were synchronized to the magnetic field pulses, because of power limitations of the pulse generator, and in order not to heat up the sample too much. Electrons emitted by the other three photon pulses

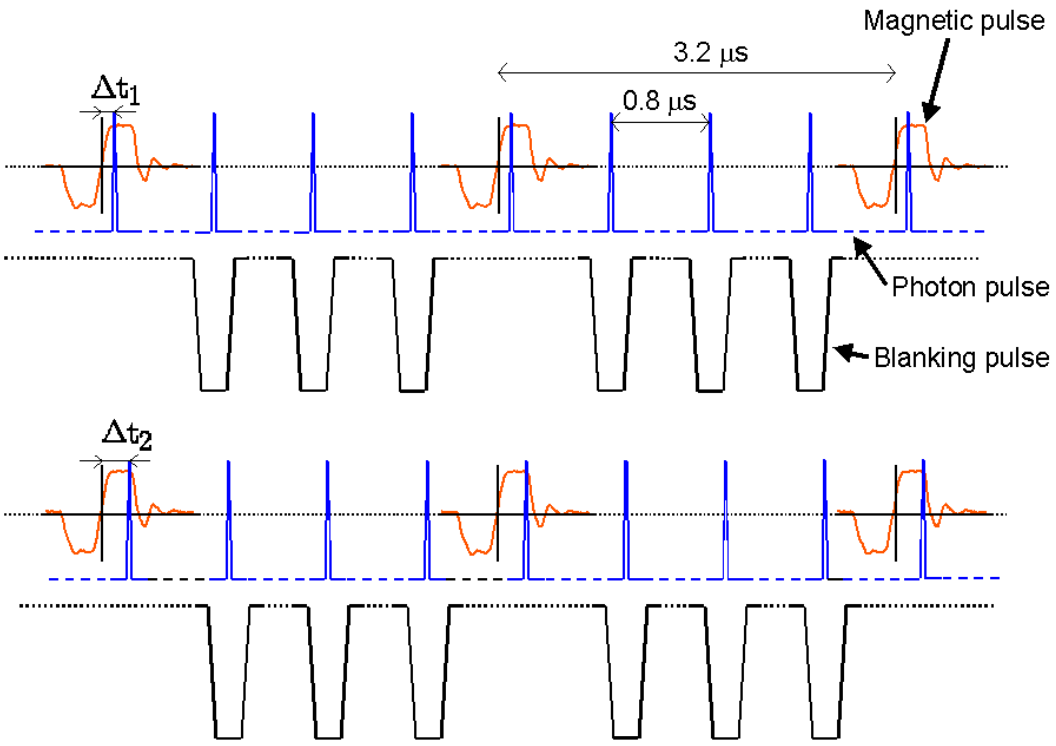

Figure 4.5: Pump-Probe scheme. The magnetic bipolar pulses (pump) were synchronized to every one out of four photon pulses (probe). Electrons emitted by the other three photon pulses were blanked out by applying a negative voltage to the energy filter (blanking pulse). Magnetization dynamics during the magnetic field pulse can be obtained by varying the pump-probe delay time, Δt.

were blocked by applying a sufficiently high negative voltage (-80 eV) to the energy filter, which is located just before the imaging unit. Photon pulses and magnetic field pulses were thus applied at 312.5 kHz. During the field pulses, magnetic domain walls in the sample are moving, and the photon pulses, which are much shorter in time (50 – 60 ps), illuminate the sample. The domain structure at that time is imaged by the camera. The width of the photon pulses represents the best time resolution. By changing the pump-probe delay time Δt, the dynamics of magnetic domain wall motion can be followed during the field pulses.

The exact position of the photon pulses with respect to the magnetic field pulse was found in the following way. The sample surface was positioned about 2 mm from the objective lens, and in between a voltage of 13 keV was applied to extract electrons from the sample surface to the objective lens. Because of the Lorentz force exerted by the magnetic field pulse, the trajectory of the electrons is deviated, and the image shifts perpendicular to the field direction. So the displacement of some surface topographic feature, for example a defect, perpendicular to the field direction

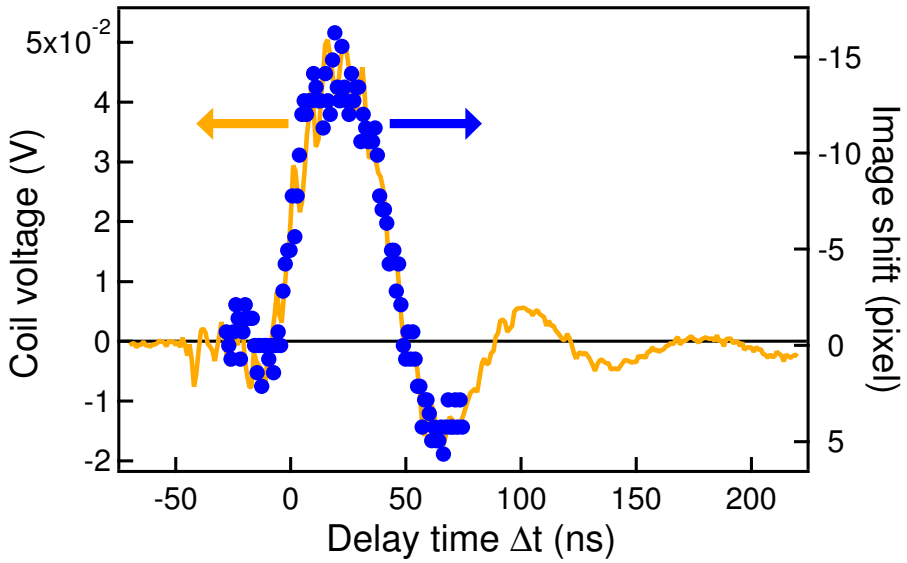

Figure 4.6: The monitored current of the pulse power supply on an oscilloscope (left axis) and the displacement of the image perpendicular to the field axis by the Lorentz force (right axis) are plotted by the solid curve and the dots, respectively, with time.

reflects the amplitude of the pulse field. This is plotted with dots in Fig. 4.6 on the right vertical axis as a function of time. The left vertical axis is the current monitor output from the pulse power supply, read on an oscilloscope. These two plots fit quite well, so the beginning of the pulse can be determined with high accuracy. No displacement of the image was observed along the field axis.